Journal of Applied Mechanics and Technical Physics, Vol. 41, No. 4, 2000

SOME CHARACTERISTICS OF HEAT AND MASS TRANSFER IN A TURBULENT AIR FLOW OVER A SURFACE

B. F. Boyarshinov

UDC 536.244

It is shown that, for a certain proportion between the rib height (2–15 mm) *installed at the test-section entrance and the turbulence level of the main flow* (1–26%), *there are extrema of parameters that describe mass transfer on the surface of an evaporating liquid fuel. In tests with and without combustion, discrete changes in the rates of heat and mass transfer are observed. Conditions for their manifestation are analyzed.*

In diffusional combustion of a condensed fuel, the intensity of heat- and mass-transfer processes can be controlled by deliberate variation of the fluctuating characteristics of the reacting boundary layer. Its stability to flameout can be achieved by installing gas-dynamic obstacles. Theoretical studies of a turbulent boundary layer with local separation face computational difficulties caused by the complex character of the flow [1, 2]. A large body of empirical information accumulated in tests without combustion [3] shows that the rates of heat and mass transfer behind an obstacle can significantly increase. However, there are differences in reported estimates of the dimensions of reattachment and relaxation flow regions and also in determined intensities of the transfer processes and their description. For a reacting boundary layer, no experimental data are available.

The objective of the present work was to experimentally study mass transfer during vaporization of a liquid fuel (ethanol) behind ribs of various heights for various turbulence levels of air streams with and without combustion.

Experimental Setup and Measurement Procedure. The tests were conducted in an open-type wind tunnel described in [4]. At the inlet of the confuser, a wire grid with a 1×1 mm-mesh or a grating with 25 threaded holes $M27 \times 1.5$ (with a 43-mm gap between the hole centers) was installed. The confuser of length $x_0 = 300$ mm (contoured according to Vitoshinskii's formula; contraction ratio 1 : 6.8) joined the test section 100×100 mm. There was no upper wall of the channel, the side walls were transparent, and the bottom wall was made of perforated plates (stainless steel). The length of the first plate was 40 mm, and that of the other six plates was 80 mm. A rib of height $h = 0$–15 mm was installed at the test-section entrance, across the entire width of the channel. The turbulence level $\mathrm{Tu}_0 = 8$, 18, or 26% was regulated by the number of open holes in the grating (25, 9, or 5, respectively); the turbulence level in tests with the grid was $\mathrm{Tu}_0 = 1\%$. These values were found by averaging the measurement results over 81 points of the entrance section spaced 10 mm apart. The measurements were performed with the help of a DISA hot-wire anemometer (single-wire probe, wire diameter 8 μm, 55M01 bridge and 55D10 linearizer). The uniformity of the air stream at the channel entrance decreased with increasing degree of turbulence, and the maximum deviation from the average (across the channel) value of the flow velocity reached $\pm 14\%$ for $\mathrm{Tu}_0 = 26\%$.

Kutateladze Institute of Thermal Physics, Siberian Division, Russian Academy of Sciences, Novosibirsk 630090. Translated from Prikladnaya Mekhanika i Tekhnicheskaya Fizika, Vol. 41, No. 4, pp. 124–130, July–August, 2000. Original article submitted October 22, 1999; revision submitted January 11, 2000.

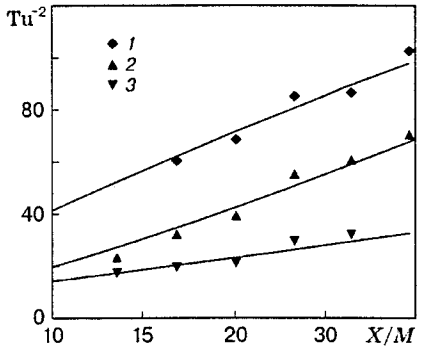

Fig. 1. Turbulence degeneration in the flow core for Tu_0 = 16 (1), 18 (2), and 26% (3).

Irrespective of the value of Tu_0, the mean (across the channel) degree of turbulence approached 8%, increasing with distance from the channel entrance, which was in line with experimentally determined limits of applicability of the pneumatic probe used, a Pitot tube with an input diameter of 1 mm, which measured total and static pressures. Outside the shear layers, on the section of length x = 0–200 mm at a distance of y = 30 mm from the wall, the rate of turbulence degeneration refers to the initial stage of turbulence development [5] (Fig. 1): $1/Tu^2 = B[X/M]^n$, where n = 0.8, 1.19, and 0.84 and B = 6.3, 1.2, and 1.85 for Tu_0 = 16, 18, and 26%, respectively, $X = x + x_0$, and the scale M = 25 mm is the inside diameter of the threaded holes in the grating. From here, following [6], we can estimate the corresponding longitudinal scales of dissipation: $L = M(X/M)^{1-0.5n}/(nB^{0.5})$.

The velocity of the turbulized air flow U_0 was regulated by the value of the dynamic pressure in the flow region with Tu $\approx$ 8% (x = 400 mm and y = 50 mm). In tests with and without combustion, the flow velocities were U_0 = 10 and U_0 = 24 m/sec, respectively. In determining the flameout velocity, the flow velocity was $U_0 < 80$ m/sec. The working liquid was 96% ethanol. The vaporization regime was adiabatic, with predominantly convective heat transfer to the surface of the liquid. In this case, the concentration of ethanol vapors at the wall does not depend on flow conditions, i.e., the mass fraction is $C_w(x) \approx$ const [4]. The values of C_w were determined from the measured surface temperature of the perforated plates using conditions on the saturation curve of an evaporating azeotropic liquid. Chromel–Alumel thermocouples with a wire diameter of 0.15 mm were welded to the center of the windward surface of each plate. It was found that, irrespective of the turbulence level, the mass fraction of ethanol vapors was C_w = 0.8 and C_w = 0.03 in tests with and without combustion, respectively. The free-stream temperature was T_0 = 290 K.

The liquid-supply system ensured a constant liquid flux through porous plates, which remained wet during the experiments. The vaporization rate of ethanol from each plate j_w was self-adjusted in accordance with the conditions of convective mass transfer. The values of j_w were determined with an accuracy of 5% from the change in the level of the liquid in measuring vessels for a certain time interval, which in tests with and without combustion was about 10 min and 3 h, respectively. From these data, the diffusional Stanton number $St_d = j_w/(\rho_0 U_0 C_w)$ was calculated. The error in determining St_d was 15%.

Experimental Results. The influence of the main determining parameters on the mass-transfer rate is illustrated in Figs. 2 and 3. In the case without combustion (Fig. 2a), the minimum deviation from the predicted dependence for a turbulent boundary layer ($St_d = 0.029\,Re_x^{-0.2}\,Sc^{-0.6}$ and Schmidt criterion Sc = 1.3) is observed for Tu_0 = 1% and h = 3 mm. For all other data, including those obtained at Tu_0 = 18–26%, there are sections with $St_d \sim Re_x^{-0.5}$ on the experimental dependences. The stratification of curves is described by the formula $St_d = \Psi_p 0.332\,Re_x^{-0.5}\,Sc^{-0.66}$, where $\Psi_p = 1.2.3.\ldots$. A similar effect was reported in [7]. The Re_x numbers at which the transition from one level to another occurs vary not only with the height of the obstacle but also with the turbulence level.

In the case with combustion (Fig. 2b), there are no discrete levels of the mass-transfer rate for Tu_0 =

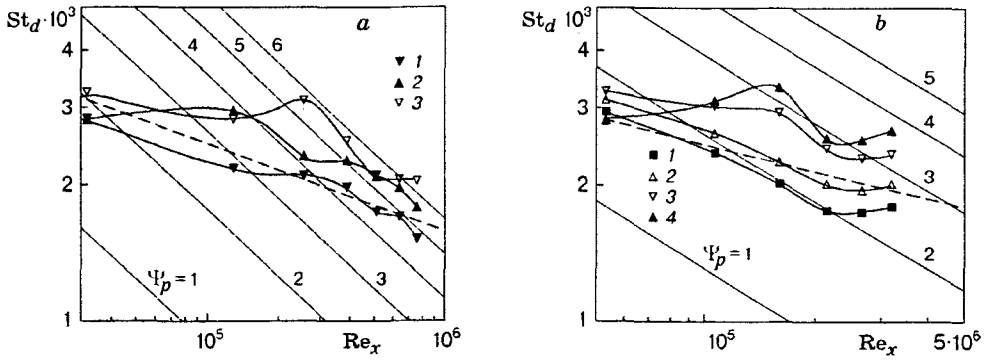

Fig. 2. Variation of the mass-transfer rate along the channel during ethanol vaporization (the dashed curve refers to $St_d = 0.029\,Re_x^{-0.2}\,Sc^{-0.6}$): (a) without combustion ($St_d = \Psi_p 0.332\,Re_x^{-0.5}\,Sc^{-0.66}$) for $Tu_0 = 1\%$ and $h = 3$ mm (1), $Tu_0 = 1\%$ and $h = 6$ mm (2), and $Tu_0 = 18\%$ and $h = 6$ mm (3); (b) with combustion ($St_d = \Psi_p 0.41\,Re_x^{-0.5}$) for $Tu_0 = 18\%$ and $h = 6$ (1), 9 (2), 12 (3), and 15 mm (4).

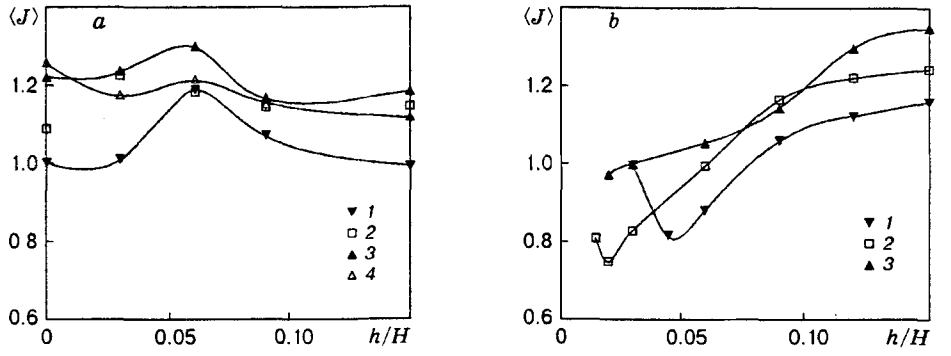

Fig. 3. Ethanol vaporization rate averaged over the channel length without combustion (a) and with combustion (b) for $Tu_0 = 1$ (1), 8 (2), 18 (3), and 26% (4).

1%, but they are observed in tests with an increased degree of turbulence. It follows from Fig. 2b that there is a jumplike increase in the burnout rate with increase in the rib height in the range $h = 6$–15 mm. This increase corresponds to the transition from the level $\Psi_p = 2$ to the level $\Psi_p = 3$. The dependence for the boundary-layer mass transfer with ethanol combustion [7] $St_d = \Psi_p 0.41\,Re_x^{-0.5}$ is shown in Fig. 2b.

In Fig. 3a, the fluxes of the substance J_w averaged over the channel length in tests without combustion are normalized to the mean flux J^* for $Tu_0 = 1\%$ and $h = 0$ (the channel height was $H = 100$ mm). Only in the case with $h = 0$ do the values of $\langle J \rangle = J_w/J^*$ increase with increasing Tu_0 throughout the whole range of turbulence studied. An increase in the mass transfer by approximately 25% is typical for tests with a turbulent boundary layer [8, 9]. For other values of h (for example, $h = 15$ mm), the difference in vaporization rates for $Tu_0 = 8$ and 26% is insignificant. In experiments, no difference between the data for $h = 0$ and $h = 15$ mm was observed for $Tu_0 = 1\%$, and at the point of the maximum ($h = 6$ mm), the averaged mass-transfer rate increases roughly by 20% (the local increase here is about 47%).

The results of tests with combustion are shown in Fig. 3b. The data were normalized by the values obtained in the experiment with vaporization and combustion for $h = 3$ mm and $Tu_0 = 1\%$. The range of the mean relative fluxes of the substance in a reacting boundary layer is seen to be wider than in the case without combustion. In tests with $Tu_0 = 1$ and 8%, minima of $\langle J \rangle$ are observed, and for $Tu_0 = 18\%$ the burnout rate increases monotonically with increasing rib height.

However, not for all values of h and Tu_0 was it possible to perform such tests. Preliminary tests with combustion in a turbulent flow showed that the region where the flame is stabilized by the rib is restricted (Fig. 4). For $Tu_0 = 1\%$ and $h < 3$ mm, the flameout was observed already at flow velocities of 3–5 m/sec,

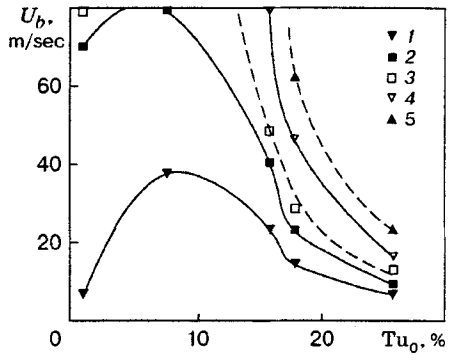

Fig. 4. Flameout velocity in combustion of evaporating ethanol in a turbulent air flow for h = 2 (1), 3 (2), 6 (3), 9 (4), and 15 mm (5).

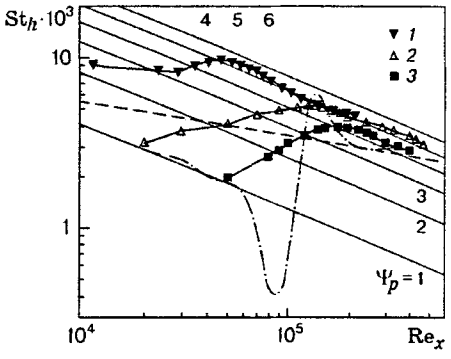

Fig. 5. Stratification of heat-transfer dependences for a turbulized boundary layer with local separation for various flow conditions and geometries: 1) blunted plate 2 cm thick (Tu_0 = 0.8% and U_0 = 8.7 m/sec) [10]; 2) rib (Tu_0 = 14.2%, U_0 = 20 m/sec, and h = 6 mm) [11]; 3) ledge (Tu_0 = 1.5%, U_0 = 20 m/sec, and h = 20 mm) [11]; the solid and dashed curves refer to $St_h = \Psi_p 0.332\,Re_x^{-0.5}\,Pr^{-0.66}$ and $St_h = 0.029\,Re_x^{-0.2}\,Pr^{-0.6}$, respectively; the dot-and-dashed curve is the calculation for a channel with a separation bubble [2].

whereas for h = 3 mm the flame is stable in a wide range of velocities, which becomes narrower with increasing turbulence level and wider with increasing rib height. The flameout velocity U_b reaches the highest value at certain values of h and Tu_0.

Discussion. Interpretation of results on boundary-layer heat and mass transfer depends on the form of their representation [4]. In the present work, the data obtained in tests with and without combustion are represented in an identical criterial treatment, since in both cases no chemical reactions proceed near the wall, and the transfer mechanism, adiabatic evaporation without injection, remains unchanged. The measurements were conducted in the same test section, whose spatial resolution was 40 and 80 mm. This resolution was determined by the length of the perforated plates and could be insufficient in the case of vaporization without combustion. It follows from Fig. 2 that the mass-transfer rates under experimental conditions with and without combustion are of the same order of magnitude, and the difference between them is caused predominantly by the special features of mass transfer in the transitional flow regime. When grids and ribs, traditional means of boundary-layer turbulence control, are used, the repeated laminarization may not vanish, but instead, it may even increase. This conclusion is confirmed by heat-transfer studies in which the spatial resolution is comparable with the thermocouple diameter.

Figure 5 shows the heat-transfer data of [10] for a blunted plate for low turbulence in the channel together with the data of [11] obtained for a flow over a rib and step for various degrees of turbulence. The results of direct numerical simulation [2] are also shown here. The separation region on the channel bottom

in [2] was formed by suction of air through a slot in the upper wall, and the input turbulence seemed to be almost zero. The results of experimental studies [$St_h = q_w/(\rho_0 U_0 C_p \Delta T)$] are stratified according to the level of intensit[illegible]7]. In a similar manner, the [illegible] of [12] for heat transfer behind a back-facing step may stratify. In [12], a by-pass (without formatio[illegible]llmien–Schlichting waves) laminar–turbulent transition was studied. The conditions for its existence a[illegible]an increased turbulence of the flow core and the presence of a closed separation region. Apparently, discrete changes in the rates of heat and mass transfer in tests with and without combustion are a characteristic feature of such a laminar–turbulent transition.

Combustion provides good visualization of the flow, due to which it was established that the flameout occurs directly behind the circulation zone, presumably at the flow reattachment point. The flameout can be reversible. In tests with $Tu_0 > 8\%$, $h > 6$ mm, and, for instance, with $U > U_b$, combustion is retained only upstream of the reattachment point. If the flow velocity is now decreased ($U < U_b$), the flame appears again throughout the entire channel length. Yarin [13] also studied the condition of flame existence, though there was no stabilization by the rib and the turbulence level was not taken into account. It was found that the flame front moves downstream as U_0 increases.

Visual observations show that there is no flame in the circulation region near the liquid. As a result, large streamwise temperature gradients can appear, which hinder the determination of C_w and St_d. Therefore, the data for the first plate in tests with combustion (see Fig. 2b) are not considered.

In tests with combustion, formation of large-scale structures can be traced, which seem to affect heat and mass transfer. Their contours in the flame are distinctly seen as bluish or yellowish regions. As the air-flow velocity increases, the vortex behind the rib become curved in several places and decomposes into loop hairpinlike structures similar to those observed in [14]. Their legs can move in the transversal direction, and their heads are fixed behind the rib. Further in time, this vortex system disintegrates with the formation of reattachment and relaxation flow regions, i.e., with the formation of a "standing wave."

It follows from visual observations that hairpinlike structures are observed in the test with $Tu_0 = 1\%$ and $h = 4.5$ mm (the minimum burnout) (see Fig. 3b). The flame front is comparatively thick, it is separated from the rib by a distance of 20–25 mm, and there are yellow features extending throughout the entire channel length. The experimental dependences St(Re) do not correspond to the levels. For $Tu_0 = 18\%$ and $h = 12$ mm, the regions with different colors approach the wall twice, and contours of an upside-down wave, or a "cycloid," are observed, two crests of which touch the surface of the perforated plates. The St(Re) dependences are stratified (see Fig. 2b). In the other minimum of the burnout velocity (see Fig. 3b: $Tu_0 = 8\%$ and $h = 2$ mm), the mass transfer is more similar to the laminar case: the Stanton numbers for four (out of seven) plates coincides with the predicted values for the case $\Psi_p = 1$. In this situation, the flame looks like a uniform blue thin sheet whose front edge is located 2–3 mm away from the rib.

In the case of vaporization without combustion, large-scale structures may be the reason for the nonmonotonic variation of mass transfer. It seems that certain combinations of U_0, Tu_0, and h are required for their formation. These structures can cause stratification of the heat-transfer data [10, 11] (see Fig. 5). They may also be responsible for the absence of the appreciable decrease in the heat-transfer rate in the flow-separation region, which is predicted by the calculations of [2]. An increase in viscosity during combustion does not prevent stratification of the mass-transfer data in a turbulized air flow. This stratification can be rather significant. For instance, for $Re_x = 2.13 \cdot 10^5$ and $Tu_0 = 8\%$, the local burnout rate increases by a factor of three as the rib height increases from 2 to 15 mm. This lends additional support to the conclusion of [15] that it is in the transition flow regime that the conditions are most favorable for controlling transfer processes.

This work was supported by the Russian Foundation for Fundamental Research (Grant No. 97-02-18520).

REFERENCES

1. H. Le, P. Moin, and J. Kim, "Direct numerical simulation of turbulent flow over a backward facing step," *J. Fluid Mech.*, **330**, No. 10, 349–376 (1997).
2. F. Spalart, M. Kh. Strelets, A. K. Travin, and M. L. Shur, "Calculation of hydrodynamics and heat transfer in a transitional separation bubble on a flat surface," in: *Proc. of the II Russian National Conf. on Heat and Mass Transfer* (Moscow, October 26–30, 1998), Vol. 2: *Forced Convection of Single-Phase Liquid*, Moscow Power-Eng. Inst., Moscow (1998), pp. 240–243.
3. T. Ota and H. Nishiyama, "Correlation of maximum turbulent heat-transfer coefficient in reattachment flow region," *Int. J. Heat Mass Transfer*, **30**, No. 6, 1193–1200 (1987).
4. B. F. Boyarshinov, É. P. Volchkov, and V. I. Terekhov, "Heat and mass transfer in a boundary layer with evaporation and combustion of ethanol," *Fiz. Goreniya Vzryva*, **30**, No. 1. 8–15 (1994).
5. J. K. Batchelor, *The Theory of Homogeneous Turbulence*, Cambridge (1953).
6. P. E. Hancock and P. Bradshaw, "The effect of free-stream turbulence on turbulent boundary layers," in: *Proc. of Am. Soc. Eng.-Mech.*: Transl. J. *Trans. ASME. J. Ser. D*, **105**, No. 3 (1983), pp. 126–133.
7. B. F. Boyarshinov, "Analysis of experimental data on heat and mass transfer in a boundary layer," *Fiz. Goreniya Vzryva*, **34**, No. 2, 73–81 (1998).
8. M. F. Blair, "Influence of free stream turbulence on turbulent boundary layer heat transfer and mean profile development. Part 2. Analysis of results," in: *Proc. of Am. Soc. Eng.-Mech.*: Transl. J. *Trans. ASME. J. Ser. C*, **105**, No. 1, 41–48 (1983).
9. A. I. Leont'ev, É. P. Volchkov, V. P. Lebedev, et al. (eds.), *Thermal Protection of Plasma-Torch Walls*, Vol. 15: *Low-Temperature Plasma* [in Russian], Inst. of Thermal Physics, Sib. Div., Russ. Acad. of Sci., Novosibirsk (1995).
10. T. Ota and N. Kon, "Heat transfer in the separated and reattached flow on a blunt flat plate," *Proc. of Am. Soc. Eng.-Mech.*: Transl. J. *Trans. ASME. J. Ser. C*, **96**, No. 4, 29–31 (1974).
11. V. I. Terekhov and N. I. Yarygina, "Heat transfer in separation regions of turbulized flows," in: *Proc. of the II Russian National Conf. on Heat and Mass Transfer* (Moscow, October 26-30, 1998), Vol. 2: *Forced Convection of Single-Phase Liquid*, Moscow Power-Eng. Inst., Moscow (1998), pp. 244–247.
12. É. Ya. Épik, L. E. Yushina, and T. T. Suprun, "Heat transfer in the relaxation region behind a local closed separation of various kinds," *ibid.*, pp. 282–285.
13. A. L. Yarin, "Detachment of the flame of a burning liquid by an air flow," *Fiz. Goreniya Vzryva*, **19**, No. 1, 3–12 (1983).
14. C. R. Smith and S. P. Schwartz, "Observation of streamwise rotation in near-wall region of turbulent boundary layers," *Phys. Fluids*, **26**, No. 3, 641–652 (1983).
15. B. F. Boyarshinov, "Study of the reasons for nonmonotonic variation of the heat-transfer rate in a boundary layer," in: *Proc. of the II Russian National Conf. on Heat and Mass Transfer* (Moscow, October 26–30, 1998), Vol. 2: *Forced Convection of a Single-Phase Liquid*, Moscow Power-Eng. Inst., Moscow (1998), pp. 66–69.